Graphene-on-Silicon Near-Field Thermophotovoltaic Cell

V. B. Svetovoy[1,2] and G. Palasantzas[3]

[1]*MESA*[+] *Institute for Nanotechnology, University of Twente, PO 217, 7500 AE Enschede, Netherlands*
[2]*Institute of Physics and Technology, Yaroslavl Branch, Russian Academy of Sciences,*
150007, Yaroslavl, Russia
[3]*Zernike Institute for Advanced Materials, University of Groningen-Nijenborgh 4,*
9747 AG Groningen, Netherlands

A graphene layer on top of a dielectric can dramatically influence the ability of the material for radiative heat transfer. This property of graphene is used to improve the performance and reduce costs of near-field thermophotovoltaic cells. Instead of low-band-gap semiconductors it is proposed to use graphene-on-silicon Schottky photovoltaic cells. One layer of graphene absorbs around 90% of incoming radiation and increases the heat transfer. This strong absorption is due to the excitation of plasmons in graphene, which are automatically tuned in resonance with the emitted light in the midinfrared range. The absorbed radiation excites electron-hole pairs in graphene, which are separated by the surface field induced by the Schottky barrier. For a quasimonochromatic source the generated power is one order of magnitude larger and the efficiency is on the same level as for semiconductor photovoltaic cells.

I. INTRODUCTION

Thermophotovoltaic (TPV) generators convert radiation emitted by a heated body into electricity [1]. In these devices a hot emitter radiates the electromagnetic energy that is absorbed by a cold photovoltaic (PV) cell (collector). In the solar TPV generators [2] solar light is absorbed and then reemitted as thermal radiation in a spectrally selective way. Any other heat source also can be used for transformation into electricity. Examples include wasted industrial heat, the heat from car engines, computer chips, etc. [3,4]. TPV systems are expected to be quiet, modular, safe, low maintenance, and pollution-free [1].

The main challenge is to increase both efficiency and output electric power of the devices. The power is restricted by the emissivity of the black body. This restriction, however, is not applicable when the bodies are separated by a distance much smaller than the thermal wavelength [5]. In this near-field range the radiative heat transfer (RHT) can be increased by orders of magnitude [6–8]. Significant enhancement of the RHT in the near field is demonstrated experimentally [9–14]. The highest efficiency is reached when the emitter is a nearly monochromatic source of radiation with the photon energy slightly larger than the band gap of the PV cell [15]. On the other hand, the strongest enhancement is realized as the resonance energy exchange when both the emitter and collector support surface modes such as plasmon or phonon polaritons matching each other [16,17]. The absorption of light by semiconductor PV cells does not have resonance character and cannot support high RHT. Moreover, TPV generators have to use narrow-band semiconductors, which are much

more expensive than silicon. In this paper, we explain how graphene could help to resolve these issues.

Graphene can add new functionalities to materials that do not have surface modes in the midinfrared (mid-IR) range [18]. This ability is because graphene supports plasmons with the frequency that is varied with the wave number, coupling constant, and Fermi level [19]. The plasmon frequency in graphene is automatically tuned with the frequency of the surface mode in the opposing body, resulting in a significant increase of the RHT [18,20]. This prediction is also confirmed experimentally [21].

Here we propose to use the graphene-on-silicon (GOS) Schottky photodiode as a PV cell. In such a generator the emitted radiation is resonantly absorbed in graphene where it excites electrons able to overcome the Schottky barrier, there is no *p-n* junction and related optical losses in the low-price Si substrate, there is no problem coupling the evanescent radiation to electrons in graphene, and the device has a simple structure. The silicon substrate is transparent in the wavelength range $\lambda = 1.2$–8.0 μm providing the optimal conditions for the RHT [18].

The GOS Schottky photodiodes were already applied for solar cells [22–24], where the visible light generated electron-hole pairs in Si separated by the surface field. The photodiode presented in Ref. [25] absorbs mid-IR light in the graphene layer and the Schottky barrier separates electrons and holes. The responsivity of the device is estimated as being at least 0.13 A/W.

Application of graphene to enhance the performance of the near-field TPV generators was already discussed. A freestanding graphene emitter is considered in combination

with the low-band-gap (0.17 eV) InSb photovoltaic cell [26]. For this device there is no resonance energy exchange between graphene and the semiconductor. A PV cell consisting of InSb substrate covered with graphene is discussed in Ref. [27], where hexagonal boron nitride (HBN) is used as the emitter. In this device the RHT is enhanced due to the resonance tuning but most of the photons are absorbed in graphene without generation of photoelectrons.

II. HEAT TRANSFER

We consider the graphene-on-silicon Schottky junction in combination with the HBN emitter that gives quasimonochromatic radiation at 0.195 eV [see Fig. 1(a)]. This specific emitter is not the point of interest as long as the photoelectrons can overcome the Schottky barrier. Moreover, a wider range of emitted frequencies is preferable. It is assumed that the bottom of the PV cell is kept at room temperature $T_c = 300$ K but the emitter temperature T_s can vary.

The energy scheme of the photodiode is shown in Fig. 1(b). Although n-type silicon is shown, p-type silicon also can be used. Infrared radiation from the emitter is absorbed in graphene providing hot electrons that are able to overcome the Schottky barrier $\Phi_b = E_F - \chi_{Si}$, where E_F is the Fermi level in graphene and χ_{Si} is the electron affinity in silicon. The surface barrier from the Si side is V_s and the forward bias applied to the diode is V. The edges of the conduction and valence bands are E_c and E_v, respectively, the Fermi level in Si is E_F^{Si}.

In contrast with the ordinary PV cells, Si is transparent for the emitted radiation. The Fermi level in pristine graphene is $E_F^0 = 4.56$ eV [28] but it can be adjusted by chemical doping of graphene in a wide range [29–31]. The barrier height has to be $\Phi_b = 0.19$ eV or lower if the HBN emitter is used. This height can be reached for n doping in graphene with the relative Fermi level $\mathcal{E}_F = E_F - E_F^0 = 0.32$ eV counted from the Dirac point. The band bending in Si is defined by the surface potential $eV_s = \Phi_b - (E_F^{Si} - E_c)$.

The photocurrent is generated by photons with the energy $\hbar\omega > \Phi_b$ absorbed in the graphene layer. The radiation of the emitter absorbed in graphene R_g can be calculated as
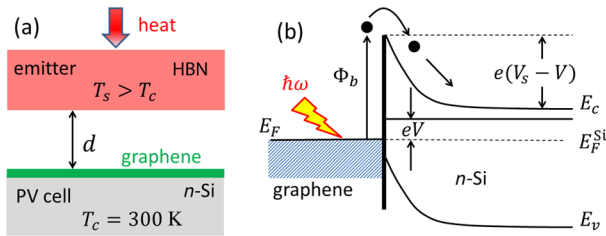

FIG. 1. (a) Schematic representation of the TPV element. (b) Energy diagram for the Schottky graphene-on-Si diode working as an infrared PV cell.

$$R_g(T_s, d) = R^-(T_s, d) - R^+(T_s, d). \quad (1)$$

Here $R^-(T_s, d)$ is the heat flux from the emitter to the collector taken in the gap just above the graphene layer. This flux is calculated as the z component of the averaged Pointing vector induced by the fluctuations in the emitter. The flux R^+ is calculated in a similar way but just below the graphene layer. These fluxes can be presented in the form

$$R^\pm(T_s, d) = \int_0^\infty \frac{d\omega}{2\pi} \hbar\omega n_B(\omega, T_s)\Pi^\pm(\omega, d), \quad (2)$$

where $n_B(\omega, T) = (e^{\hbar\omega/T} - 1)^{-1}$ is the Bose factor (the Boltzmann constant here is $k_B = 1$). The evanescent spectral function $\Pi^-(\omega, d)$ is

$$\Pi^-(\omega, d) = \int \frac{d^2q}{(2\pi)^2} \frac{4\mathrm{Im}r_c\mathrm{Im}r_s e^{-2qd}}{|1 - r_s r_c e^{-2qd}|^2}. \quad (3)$$

Here, r_s and r_c are the reflection coefficients of the source and collector, respectively, which are functions of ω and the wave vector $\mathbf{q}$ parallel to the plates. The result for $\Pi^-(\omega, d)$ is well known [5,8,16,17], but the expression for $\Pi^+(\omega, d)$ has to be calculated. It can be done using the standard approach of fluctuational electrodynamics. Skipping the details, the final expression for the spectral function $\Pi_g = \Pi^- - \Pi^+$ is

$$\Pi_g(\omega, d) = \int \frac{d^2q}{(2\pi)^2} \frac{4\mathrm{Im}\varepsilon_g\mathrm{Im}r_s|1 - r_c|^2 e^{-2qd}}{|1 - r_s r_c e^{-2qd}|^2}, \quad (4)$$

where $\varepsilon_g(\omega, q)$ is the dielectric function of graphene and κ is the average dielectric constant of the media above and below the graphene layer.

Graphene is responsible for the energy exchange in the system. Without graphene on top of silicon the heat transfer is negligible because Si is transparent for the emitted radiation. It is known that the effect of graphene can be evaluated with a good precision ($\sim\alpha = e^2/\hbar c$) in the nonretarded limit $c \to \infty$ [18,32,33], where only p-polarized evanescent fluctuations contribute to the momentum or energy exchange between parallel plates separated by a submicrometer gap. Therefore, in Eqs. (2)–(4) it is sufficient to take into account only the contribution of p-polarized evanescent waves.

In order to calculate the total energy exchange between bodies we have to include the heat flux going to the emitter and originating from fluctuations in the collector. Normally it can be done by the substitute in Eq. (2)

$$n_B(\omega, T_s) \to N(\omega, T_s, T_c) = n_B(\omega, T_s) - n_B(\omega, T_c), \quad (5)$$

because in the thermal equilibrium $T_s \to T_c$ the total RHT has to be zero [5]. However, the procedure is different if the collector is used as a PV element. As for semiconductors

[34,35] the potential difference V results in nonthermal photons that have nonzero chemical potential $\mu_{ph} = eV$ but still can be described by the collector temperature T_c. This is true for photons with the energy above the Schottky barrier $\hbar\omega > \Phi_b$; the photons with smaller energies have $\mu_{ph} = 0$. In this case the thermal factor $N(\omega, T_s, T_c)$ is defined as

$$N(\omega, T_s, T_c) = n_B(\omega, T_s) - n_B(\omega - \mu_{ph}/\hbar, T_c), \quad (6)$$

where we have to understand μ_{ph} as a discontinuous function of ω

$$\mu_{ph}(\omega) = \begin{cases} 0, & \hbar\omega < \Phi_b; \\ eV, & \hbar\omega > \Phi_b. \end{cases} \quad (7)$$

The final result for the radiative power P_{rad} per unit area is

$$P_{rad}(d, T_s, T_c) = \int_0^\infty \frac{d\omega}{2\pi} \hbar\omega N(\omega, T_s, T_c)\Pi^-(\omega, d). \quad (8)$$

It is similar to the expression used in Refs. [26,27]. The difference is that in our case the collector emits radiation with $\hbar\omega < \Phi_b$ due to the presence of graphene, while for a semiconductor PV cell with the band gap E_{gap} the adopted approximation is that the radiation with $\hbar\omega < E_{gap}$ is not emitted. The radiative power absorbed in the graphene layer P_g can be calculated from Eq. (8) with the substitute $\Pi^- \to \Pi_g$.

III. GENERATED POWER

Let us assume first that each photon with the energy above Φ_b which is absorbed in graphene produces one electron in the conduction band of Si. The actual responsivity of the photodiode will be discussed later. In this case the photocurrent generated in the cell [15] is

$$I_{ph}(V) = e \int_{\Phi_b/\hbar}^\infty \frac{d\omega}{2\pi} N(\omega, T_s, T_c)\Pi_g(\omega, d). \quad (9)$$

It is proportional to the number of photons with the energy above Φ_b absorbed in graphene. The generated electrical power and efficiency of the cell are defined as

$$P_{PV} = VI_{ph}(V), \qquad \eta = P_{PV}/P_{rad}, \quad (10)$$

where P_{PV} is similar to that used in Refs. [26,27]. Note that η does not include the efficiency of heating of the emitter and the efficiency of light transformation by the photodiode. The electric power is zero for $V = 0$ corresponding to the short circuit and for $V = (1 - T_c/T_s)\Phi_b/e$ corresponding to the open-circuit voltage. The maximal power is realized somewhere in between these values.

The dielectric function of the emitter is described by the Drude-Lorentz model

$$\varepsilon_{HBN}(\omega) = \varepsilon_\infty \left(1 + \frac{\omega_L^2 - \omega_T^2}{\omega_T^2 - \omega^2 - i\Gamma\omega}\right), \quad (11)$$

with the parameters of HBN from Ref. [36] $\varepsilon_\infty = 4.88$, $\omega_L = 0.2$ eV, $\omega_T = 0.17$ eV, and $\Gamma = 0.66 \times 10^{-3}$ eV. The reflection coefficient of the emitter (p polarization, nonretarded) $r_s = (\varepsilon_{HBN} - 1)/(\varepsilon_{HBN} + 1)$ has a surface phonon-polariton resonance at 0.195 eV.

The reflection coefficient of the collector r_c can be presented in the form

$$r_c = \frac{\varepsilon_{Si} - 1 + 2\kappa(\varepsilon_g - 1)}{\varepsilon_{Si} + 1 + 2\kappa(\varepsilon_g - 1)}, \quad (12)$$

where $\varepsilon_{Si} \approx 11.9$ is practically a constant for Si in mid-IR and $\varepsilon_g(\omega, q)$ is the dielectric function of graphene. In the limit of small relaxation frequency $\gamma \to 0$ the latter can be presented in the form

$$\varepsilon_g(\omega, q) = 1 + \frac{4\alpha_g \mathcal{E}_F}{\hbar v_F q}\left(1 - \frac{\omega}{\sqrt{\omega^2 - v_F^2 q^2}}\right), \quad (13)$$

where $\alpha_g = e^2/\kappa\hbar v_F$ is the coupling constant and v_F is the Fermi velocity in graphene. Equation (13) can be applied in the range $q < 2T/\hbar v_F$; finite γ can be accounted for with the substitute $\omega \to \omega + i\gamma$ and some nonessential modification of ε_g (see Refs. [18,20] for details).

The spatial dispersion of ε_g is an important property. It results in the plasmon frequency that depends on q even in the nonretarded limit

$$\hbar\omega_p(q) \approx (2\alpha_g \hbar v_F q \mathcal{E}_F)^{1/2}. \quad (14)$$

This dependence means that for a body covered with graphene, one can always find a value of q that gives the plasmon resonance matching the surface mode in the opposite body. When the substrate permittivity is large, graphene gives only a small correction to r_c and there will be no significant increase in RHT. For silicon it is rather large but even a thin native oxide ($h \sim 1$ nm) on Si influences the reflection coefficient. We take this oxide into account in our calculations and use the graphene relaxation frequency $\gamma = 33$ meV (5×10^{13} rad/s).

The results are shown in Fig. 2. First, using Eq. (10) the output power is maximized by varying the operating voltage of the cell V. The theoretical limit of this voltage $V < (1 - T_c/T_s)\Phi_b/e$ and the value found from the maximization of P_{PV} at $d = 10$ nm are shown in Fig. 2(a) as functions of the emitter temperature. The optimal value of V varies only slightly with the distance. The net radiative power P_{rad} and the power absorbed in graphene P_g are shown in Fig. 2(b). The curves nearly coincide because
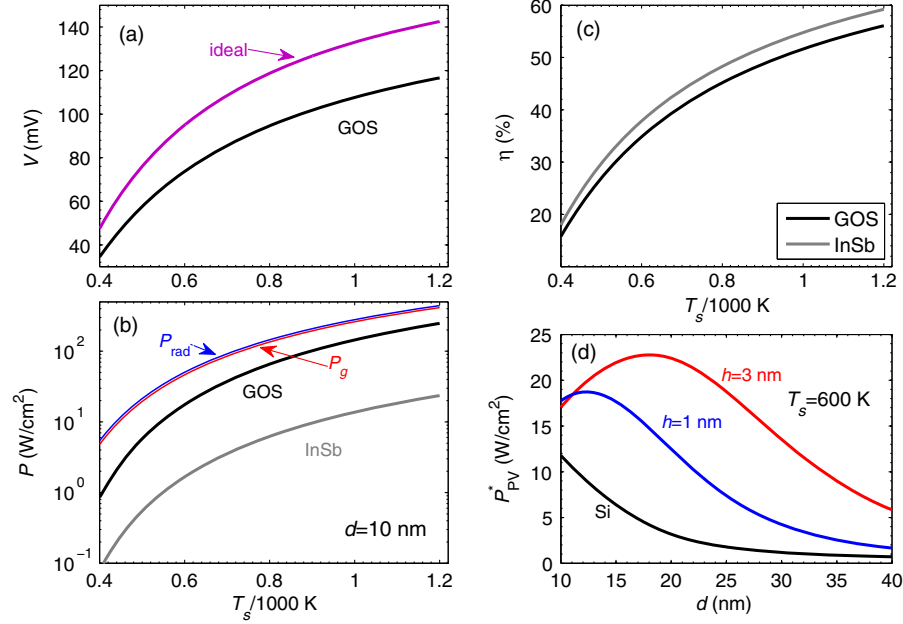
FIG. 2. (a) The theoretical limit on the operating voltage (ideal) and the voltage maximizing P_{PV} for the GOS cell as functions of T_s. (b) The radiative (blue) and absorbed in graphene (red) powers as functions of temperature. The output power for the GOS cell and InSb cell are presented as black and gray curves, respectively. (c) Efficiency of the TPV elements as a function of temperature. (d) Dependence of the scaled output power on the distance for different thicknesses of the SiO$_2$ layer on Si including bare substrate.

about 90% of incoming radiation is absorbed in graphene. This exceptional phenomenon is the result of plasmon excitation in resonance with the radiation of the emitter. The output power of the cell is also presented in Fig. 2(b). For comparison, P_{PV} for the InSb PV cell is shown too, which is one order of magnitude smaller. The efficiency for the GOS cell shown in Fig. 2(c) is somewhat smaller than that for the InSb cell. It happens because 90% of the light incoming on the GOS cell generates photocarriers, while it is assumed that 100% of the light generates carriers in the semiconductor cell. The latter, of course, is not true because to contribute to the photocurrent, the electron-hole pairs have to reach the depletion layer before recombination [37,38]. We can conclude that the TPV element with the graphene-on-Si Schottky PV cell can outperform semiconductor PV cells if the responsivity of the Schottky photodiode will be comparable with that of low-band-gap semiconductors.

The dependence of the scaled output powers $P_{PV}^* = P_{PV}(d/10 \text{ nm})^2$ on the distance d is shown in Fig. 2(d) for three different thicknesses of the SiO$_2$ layer on Si. All the curves are presented for $T_s = 600$ K. At the maximum the frequency of plasmon (14) matches the resonance in the emitter $\hbar\omega_p(q) \approx 0.195$ eV at $q \approx 1/2d$. Deviation from this relation in any direction will result in a decrease of the scaled power. Graphene on a thin silicon-oxide film corresponds to some intermediate situation between pure Si and pure SiO$_2$.

For low barrier height the surface electric field at high T_s becomes too small to separate the carriers (the same

problem exists for low-band-gap semiconductors). It is therefore interesting to analyze the behavior of the GOS cell for different barrier heights. To perform this analysis we model the emitter with the dielectric function similar to Eq. (11) but with the parameters $\varepsilon_\infty = 5$, $(\omega_L/\omega_T)^2 - 1 = 0.5$, $\Gamma/\omega_T = 5 \times 10^{-3}$, which are close to those for HBN. The resonance frequency of the reflection coefficient

$$\omega_r = \omega_T[\varepsilon_{em}(0) + 1]^{1/2}(\varepsilon_\infty + 1)^{-1/2} \qquad (15)$$

is the varied parameter, where $\varepsilon_{em}(0)$ is the static permittivity of the emitter. It is assumed that the barrier height is somewhat smaller than ω_r. Some results are shown in Fig. 3. The left panel shows that the output power is smaller for higher barrier at low T_s but becomes comparable or even larger at high T_s as the curves 1 and 2 demonstrate. However, when the barrier is too high, P_{PV} becomes smaller at all temperatures. The reason is that the value of the momentum q in Eq. (14) for which $\hbar\omega_p > \Phi_b$ becomes significantly larger than $1/2d$. It reduces the radiative power due to the factor e^{-2qd} and results in the decrease of P_{PV}. The output power produced by the InAs PV cell with the band gap 0.36 eV is shown for comparison in the same panel. The right panel shows the fraction of the radiative power absorbed in graphene for different barrier heights. This fraction is always large especially at high T_s. It is somewhat smaller at low temperatures and high barriers.
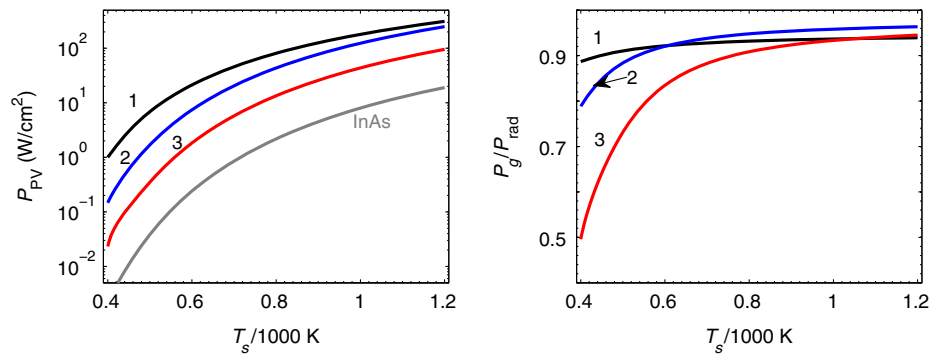
FIG. 3. (left) The output power at $d = 10$ nm as a function of temperature for different barrier heights. The curves 1, 2, and 3 correspond to the barriers 0.18, 0.28, and 0.33 eV, respectively. The emitter resonance frequency is 0.02 eV higher in all cases. The gray curve shows the result for InAs PV cell. (right) Fraction of the incident radiation absorbed in the graphene layer for different barrier heights.

Dependence on the barrier height demonstrates that the GOS PV cell is able to support plasmons in the mid-IR range where it is superior over the semiconductor PV cells. At shorter wavelengths $\lambda < 3.5$ μm the radiative heat exchange is significantly reduced and the GOS cell loses its advantages.

IV. DISCUSSION

Up to now we assumed that the photodetector is perfect. The typical responsivity of low-band-gap semiconductors is 1 A/W. It is still larger than the reported value 0.13 A/W [25] for the GOS Schottky photodiode. However, the main problem of graphene-based photodetectors is the coupling of light with graphene. For incoming propagating waves absorption in graphene is small $\sim\alpha$. To increase the responsivity one has to couple light with sophisticated optical structures (see Ref. [25] and references therein). These structures inevitably add losses reducing the effective responsivity. Additionally, the graphene-Si junction is not optimized. The configuration used in our scheme does not suffer from the coupling problem because the heat transfer is realized via the evanescent waves, for which we find that 90% of incoming radiation is absorbed in a single graphene layer. Therefore, the responsivity for our configuration can be increased well above 0.13 A/W.

At this moment control of the gap in a few tens of nanometers between parallel plates is a very challenging problem. However, progress in this direction is fast. The distances 30–60 nm are already explored for RHT experimentally [21,39,40] in the sphere-plate configuration. In the parallel-plates configuration the heat transfer is investigated at distances up to 1 μm [41,42]. Large parallel plates separated by a distance of 100 nm or smaller are also an important problem for many micromechanical applications and it is actively investigated [43,44]. For this reason we hope that our proposition can be a reality in the near future.

V. CONCLUSIONS

We considered the near-field TPV element having as a PV cell graphene-on-silicon Schottky photodiode. Because of the presence of graphene, this PV cell has resonant heat exchange with the emitter; a single layer of graphene absorbs 90% of incoming radiation that can be efficiently transformed to photocurrent. Already for the quasimonochromatic emitter the device demonstrates well-advanced characteristics.

[1] T. J. Coutts, An overview of thermophotovoltaic generation of electricity, Sol. Energy Mater. Sol. Cells **66,** 443 (2001).

[2] A. Lenert, D. M. Bierman, Y. Nam, W. R. Chan, I. Celanovic, M. Soljačić, and E. N. Wang, A nanophotonic solar thermophotovoltaic device, Nat. Nanotechnol. **9,** 126 (2014).

[3] S. Basu, Z. M. Zhang, and C. J. Fu, Review of near-field thermal radiation and its application to energy conversion, Int. J. Energy Res. **33,** 1203 (2009).

[4] M. Bosi, C. Ferrari, M. Franceso, M. Pinelli, P. R. Spina, and M. Venturini, Thermophotovoltaic generation: A state of the art review, in *Proceedings of the International Conference on Efficiency, Cost, Optimization, Simulation and Envinromental Impact of Energy Systems, 2012*, edited by U. Desideri, G. Manfrida, and E. Sciubba (Firenze University, Perugia, 2012), p. 258.

[5] D. Polder and M. Van Hove, Theory of radiative heat transfer between closely spaced bodies, Phys. Rev. B **4,** 3303 (1971).

[6] J. B. Pendry, Radiative exchange of heat between nanostructures, J. Phys. Condens. Matter **11,** 6621 (1999).

[7] C. H. Park, H. A. Haus, and M. S. Weinberg, Proximity-enhanced thermal radiation, J. Phys. D **35,** 2857 (2002).

[8] J.-P. Mulet, K. Joulain, R. Carminati, and J.-J. Greffet, Enhanced radiative heat transfer at nanometric distances, Microscale Thermophys. Eng. **6**, 209 (2002).

[9] C. Hargreaves, Anomalous radiative transfer between closely spaced bodies, Phys. Lett. A **30**, 491 (1969).

[10] A. Kittel, W. Müller-Hirsch, J. Parisi, S.-A. Biehs, D. Reddig, and M. Holthaus, Near-field heat transfer in a scanning thermal microscope, Phys. Rev. Lett. **95**, 224301 (2005).

[11] L. Hu, A. Narayanaswamy, X. Chen, and G. Chen, Near-field thermal radiation between two closely spaced glass plates exceeding Plancks blackbody radiation law, Appl. Phys. Lett. **92**, 133106 (2008).

[12] A. Narayanaswamy, S. Shen, and G. Chen, Near-field radiative heat transfer between a sphere and a substrate, Phys. Rev. B **78**, 115303 (2008).

[13] S. Shen, A. Narayanaswamy, and G. Chen, Surface phonon polaritons mediated energy transfer between nanoscale gaps, Nano Lett. **9**, 2909 (2009).

[14] E. Rousseau, A. Siria, G. Jourdan, F. Comin, J. Chevrier, and J.-J. Greffet, Radiative heat transfer at the nanoscale, Nat. Photonics **3**, 514 (2009).

[15] M. Laroche, R. Carminati, and J.-J. Greffet, Near-field thermophotovoltaic energy conversion, J. Appl. Phys. **100**, 063704 (2006).

[16] K. Joulain, J.-P. Mulet, F. Marquier, R. Carminati, and J.-J. Greffet, Surface electromagnetic waves thermally excited: Radiative heat transfer, coherence properties and Casimir forces revisited in the near field, Surf. Sci. Rep. **57**, 59 (2005).

[17] A. I. Volokitin and B. N. J. Persson, Near-field radiative heat transfer and noncontact friction, Rev. Mod. Phys. **79**, 1291 (2007).

[18] V. B. Svetovoy, P. J. van Zwol, and J. Chevrier, Plasmon enhanced near-field radiative heat transfer for graphene covered dielectrics, Phys. Rev. B **85**, 155418 (2012).

[19] M. Jablan, H. Buljan, and M. Soljačić, Plasmonics in graphene at infrared frequencies, Phys. Rev. B **80**, 245435 (2009).

[20] O. Ilic, M. Jablan, J. D. Joannopoulos, I. Celanović, H. Buljan, and M. Soljačić, Near-field thermal radiation transfer controlled by plasmons in graphene, Phys. Rev. B **85**, 155422 (2012).

[21] P. J. van Zwol, S. Thiele, C. Berger, W. A. de Heer, and J. Chevrier, Nanoscale radiative heat flow due to surface plasmons in graphene and doped silicon, Phys. Rev. Lett. **109**, 264301 (2012).

[22] X. Li, H. Zhu, K. Wang, A. Cao, J. Wei, C. Li, Y. Jia, Z. Li, X. Li, and D. Wu, Graphene-on-silicon Schottky junction solar cells, Adv. Mater. **22**, 2743 (2010).

[23] Y. Ye and L. Dai, Graphene-based Schottky junction solar cells, J. Mater. Chem. **22**, 24224 (2012).

[24] X. Miao, S. Tongay, M. K. Petterson, K. Berke, A. G. Rinzler, B. R. Appleton, and A. F. Hebard, High efficiency graphene solar cells by chemical doping, Nano Lett. **12**, 2745 (2012).

[25] X. Wang, Z. Cheng, K. Xu, H.-K. Tsang, and J.-B. Xu, High-responsivity graphene/silicon-heterostructure waveguide photodetectors, Nat. Photonics **7**, 888 (2013).

[26] O. Ilic, M. Jablan, J. D. Joannopoulos, I. Celanovic, and M. Soljačić, Overcoming the black body limit in plasmonic and graphene near-field thermophotovoltaic systems, Opt. Express **20**, A366 (2012).

[27] R. Messina and P. Ben-Abdallah, Graphene-based photovoltaic cells for near-field thermal energy conversion, Sci. Rep. **3**, 1383 (2013).

[28] R. Yan, Q. Zhang, W. Li, I. Calizo, T. Shen, C. A. Richter, A. R. Hight-Walker, X. Liang, A. Seabaugh, D. Jena, H. G. Xing, D. J. Gundlach, and N. V. Nguyen, Determination of graphene work function and graphene-insulator-semiconductor band alignment by internal photoemission spectroscopy, Appl. Phys. Lett. **101**, 022105 (2012).

[29] H. K. Jeong, K.-J. Kim, S. M. Kim, and Y. H. Lee, Modification of the electronic structures of graphene by viologen, Chem. Phys. Lett. **498**, 168 (2010).

[30] Y. Yi, W. M. Choi, Y. H. Kim, J. W. Kim, and S. J. Kang, Effective work function lowering of multilayer graphene films by subnanometer thick AlO_x overlayers, Appl. Phys. Lett. **98**, 013505 (2011).

[31] Y. Shi, K. K. Kim, A. Reina, M. Hofmann, L.-J. Li, and J. Kong, Work function engineering of graphene electrode via chemical doping, ACS Nano **4**, 2689 (2010).

[32] G. Gómez-Santos, Thermal van der Waals interaction between graphene layers, Phys. Rev. B **80**, 245424 (2009).

[33] V. B. Svetovoy, Z. Moktadir, M. C. Elwenspoek, and H. Mizuta, Tailoring the thermal Casimir force with graphene, Europhys. Lett. **96**, 14006 (2011).

[34] P. Würfel, The chemical potential of radiation, J. Phys. C **15**, 3967 (1982).

[35] A. Luque and A. Martí, in *Handbook of Photovoltaic Science and Engineering*, edited by A. Luque and S. Hegedus (John Wiley & Sons, New York, 2003).

[36] A. Narayanaswamy and G. Chen, Surface modes for near field thermophotovoltaics, Appl. Phys. Lett. **82**, 3544 (2003).

[37] K. Park, S. Basu, W. P. King, and Z. M. Zhang, Performance analysis of near-field thermophotovoltaic devices considering absorption distribution, J. Quant. Spectrosc. Radiat. Transfer **109**, 305 (2008).

[38] M. Francoeur, R. Vaillon, and M. P. Mengüç, Thermal impacts on the performance of nanoscale-gap thermophotovoltaic power generators, IEEE Trans. Energy Convers. **26**, 686 (2011).

[39] S. Shen, A. Mavrokefalos, P. Sambegoro, and G. Chen, Nanoscale thermal radiation between two gold surfaces, Appl. Phys. Lett. **100**, 233114 (2012).

[40] J. Shi, P. Li, B. Liu, and S. Shen, Tuning near field radiation by doped silicon, Appl. Phys. Lett. **102**, 183114 (2013).

[41] R. S. Ottens, V. Quetschke, S. Wise, A. A. Alemi, R. Lundock, G. Mueller, D. H. Reitze, D. B. Tanner, and B. F. Whiting, Near-field radiative heat transfer between macroscopic planar surfaces, Phys. Rev. Lett. **107**, 014301 (2011).

[42] T. Kralik, P. Hanzelka, M. Zobac, V. Musilova, T. Fort, and M. Horak, Strong near-field enhancement of radiative heat transfer between metallic surfaces, Phys. Rev. Lett. **109**, 224302 (2012).

[43] M. B. Syed Nawazuddin, Ph.D. thesis, University of Twente, 2013.

[44] D. N. Woolf, Ph.D. thesis, Harvard University, 2013.